

The effect of wall linings and door lamination on photoneutron dose distribution around linear medical accelerators

F. Azairi, J. Ghassoun*, R. Bechchar, S. Harif, S. Kabrane

EPRA, Department of physics, Faculty of Sciences Semlalia, Marrakech, Morocco

ABSTRACT

► Original article

***Corresponding author:**

Jillali Ghassoun, Ph.D.,
E-mail: ghassoun@uca.ac.ma

Received: July 2023

Final revised: October 2024

Accepted: November 2024

Int. J. Radiat. Res., April 2025;
23(2): 413-420

DOI: [10.61186/ijrr.23.2.21](https://doi.org/10.61186/ijrr.23.2.21)

Keywords: Radiotherapy, radiation shielding, neutrons, gamma rays, Monte Carlo method.

Background: The aim of this study is to investigate the shielding effect of the internal wall linings and laminated shield door on photoneutron and capture gamma doses at the isocenter and at the maze entrance of radiotherapy treatment rooms.

Material and Methods: The Monte Carlo N-Particle Transport (MCNP5) code was used to simulate the radiotherapy room within a medical linear accelerator operating at 12, 15, 18, and 25 MV. The energy spectra of neutron and secondary gamma rays, with their corresponding dose equivalents, were calculated inside the bunker and at various points along the maze. To verify the accuracy of our Monte Carlo simulation, we compared our findings with those obtained through analytical methods recommended by (IAEA) safety report No.47. Once validated, the Monte Carlo simulation was used for assessing dose reduction by the room wall linings and the laminated shield door. **Results:** Our results showed that the use of paraffin wax infused with boron carbide within the lining of radiotherapy room walls reduces doses of both neutron and capture gamma radiation at the isocenter by up to 13% and 35.9%, respectively. However, the laminated shield door reduced significantly both neutron and capture gamma dose equivalents near the bunker door by up to 99.75% and 38.20%, respectively. **Conclusion:** The obtained results show that the use of neutron shielding material in the lining of the radiotherapy wall rooms reduces neutron and capture gamma radiation doses to the patient. While, the laminated shield door presents enough effectiveness in protecting the workers and general public.

INTRODUCTION

High-energy photon beams are widely used in new radiotherapy techniques to improve the quality of the treatment of deep-seated tumors ⁽¹⁾. However, medical linear accelerators operating above 10 MV present a significant radiation protection problem. Indeed, it produces undesirable photoneutrons by the interaction of high energy photons with high density materials, and principally, through the Giant Dipole Resonance (GDR) in the nuclear reactions with high-Z materials constituting the medical linear accelerators head (W, Cu, Fe, and Pb) ^(2,3).

These photoneutrons may also generate secondary gamma rays, by capture and inelastic reactions, which increase the risk of undesired dose to the patient, the oncology staff, and the general public. On the other hand, the Treatment Planning Systems (TPS) do not take into account the photoneutron dose and its associated biological effects ^(4,5).

So the National Commission on Radiation Protection and Measurements (NCRP) No. 151 ⁽⁶⁾, and the International Atomic Energy Agency (IAEA)

Safety Report No. 47 ⁽⁷⁾ have recommended that the photoneutron and capture gamma rays must be considered. Inside the bunkers with linacs operating at energies greater than 10 MV. To decrease the radiation dose near the bunker door, a maze must be incorporated into the design of radiotherapy facilities.

Yücel *et al.* ⁽⁸⁾ measured the neutron dose for 18 MV linac at the patient's position and concluded that such a dose should not be considered as negligible. Therefore, they proposed to use neutron-absorbing protective materials during treatment.

In our previous work ⁽⁹⁾, the Monte Carlo method was used to model a radiotherapy room of a medical linear accelerator operating at 18 MV and to estimate the neutron and the secondary gamma ray dose equivalents inside the radiotherapy room and along the maze. Moreover, the neutron and the capture gamma fluences, the energy spectra, and the dose equivalent distributions were even studied in a tissue equivalent phantom representing a patient's body ⁽¹⁰⁾. In addition, the effect of the wall linings and the maze with various materials for neutron shield was also investigated. It was concluded that the wall linings

with paraffin wax incorporating boron carbide can significantly decrease doses from both neutron and secondary gamma radiation within the treatment room and at the entrance to the maze, for medical linear accelerator operating at 18 MV⁽¹¹⁾. The study of Wang *et al.*⁽¹²⁾ showed a notable reduction in neutron and secondary gamma ray exposure at the maze entrance using borated polyethylene (BPE) boards as neutron absorption lining materials. Afkham *et al.*⁽¹³⁾ focused on developing an efficient shielding material for fast neutrons in medical linear accelerators, using the nanoparticles of Fe₃O₄ and B₄C in a matrix of silicone resin. Mesbahi *et al.*⁽¹⁴⁾ studied the influence of treatment room and maze layout on photoneutron and capture gamma dose equivalents.

In this work, the effect of neutron shielding material lining the radiotherapy room walls and the laminated shield door on radiation dose was investigated in order to determine the most adequate one of them. The Monte Carlo method was used to model a radiotherapy room of a medical linear accelerator operating at 12, 15, 18, and 25 MV and to evaluate the shielding effectiveness of these shields. The calculations were performed in the absence and the presence of wall linings, then in the existence of a laminated shield door located at the maze entrance. The effect of these shields was quantified in terms of dose equivalent reduction of both neutrons and capture gamma rays.

MATERIALS AND METHODS

Monte Carlo simulation

The Monte Carlo (MC) method was employed to model a medical linacs operating at 12, 15, 18, and 25 MV (Saturne linac 43). The simulations were carried out using the MCNP5 Monte Carlo Code⁽¹⁵⁾. In our Monte Carlo simulation, 10⁹ histories were run to achieve an estimated relative error of less than 2%. The neutron and gamma ray doses were calculated using fluence-to-dose equivalent conversion coefficients from NCRP-38⁽¹⁶⁾ and ICRP-74⁽¹⁷⁾.

Figure (1.a) illustrates the floor plan depiction of the simulated radiotherapy room and the points around radiation dose equivalents, which are tallied. Our assumption considered All surfaces, including the walls, floor, and ceiling, are constructed of ordinary concrete⁽¹⁸⁾. The height from the floor to the ceiling was 2.7 m. The neutron and capture gamma fluences and dose equivalent were calculated in spherical cells with a diameter of 10 cm at different locations using the track length estimator (tally type F4). A height of 114 cm from the floor was considered as the position of all the points.

In order to investigate the shielding effect of the laminated shield door and the internal wall linings and to determine the most adequate one of them, a

series of calculation were performed. The shielding effect was evaluated by comparing the results at the isocenter and the outer maze entrance door (point H in figure 1a), for three cases (figure 1b):

Case (I): the walls of the radiotherapy room are constructed of 1 meter of concrete in the absence of shielding door and wall linings.

Case (II): the room walls are lined with paraffin wax containing boron carbide as a neutron absorption material.

Case (III): it is the same as in case (I) but it has a laminated shield door at the maze entrance.

The laminated shield door consists of four shielding layers (figure1a): a 10.2 cm thick layer of borated polyethylene, BPE (5% boron) and a 1.27 cm thick layer of lead sandwiched between two steel layers (0.635 cm)⁽¹⁹⁾. Adding boron to materials like polyethylene enhances the thermal neutron capture, because of its high capture cross section. The layer of lead, placed after the borated polyethylene, serves to attenuate gamma radiation.

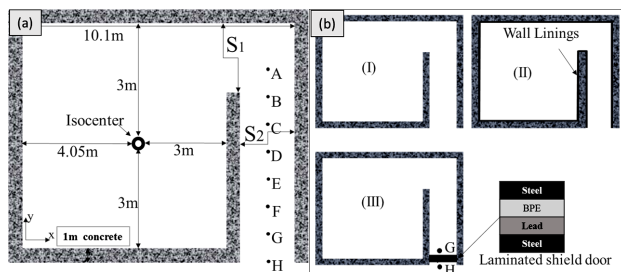


Figure 1. The plan view of the radiation therapy room and points around which radiation dose equivalents are tallied (a), and the treatment layouts used in the current study. (I): without door and without wall linings, (II): with wall linings, (III): with door (b).

The source energy spectrum

A tungsten sphere with a radius of 10 centimeters was used to simulate the accelerator head with an air conical aperture around the source where neutrons are produced. The source is described as an isotropic point-like source energy spectrum given by equation (1)⁽²⁰⁾:

$$\frac{dN}{dE_n} = \frac{0.8929E_n}{T^2} \exp\left(-\frac{E_n}{T}\right) + \frac{0.1071 \ln\left(\frac{E_{max}}{E_n + 7.34}\right)}{\int_0^{E_{max}} \ln\left(\frac{E_{max}}{E_n + 7.34}\right) dE_n} \quad (1)$$

here E_{max} is the maximum energy of the photons (in MeV), E_n is the energy of neutrons (in MeV) and T is the nuclear temperature (in MeV) of the target material.

Neutron dose equivalent

To verify the accuracy of our Monte Carlo simulations, we compared our findings with those obtained through analytical methods by the IAEA Report No. 47⁽⁷⁾. In this work, the modified Kersey method proposed by Wu-McGinley⁽²¹⁾ was selected as the benchmark for the comparison^(10, 12). The neutron dose equivalent ($H_{n,D}$) is defined by the following equation 2:

$$H_{n,D} = 2.4 \times 10^{-15} \times \varphi_A \times \sqrt{\frac{S_1}{S_2}} \times (1.64 \times 10^{\frac{-d_2}{1.9}} + 10^{\frac{-d_2}{TVD}}) \quad (2)$$

Where d_2 is the distance between point A and the outer entrance of the maze (point H in figure 1a), S_1/S_2 represents the proportion of the cross-sectional area of the inner maze to that of the outer maze, TVD is the tenth value length given by equation 3 (7):

$$TVD = 2.06\sqrt{S_2} \quad (3)$$

And φ_A represents the total neutron fluence, at the inner maze (point A), per photon Gray at the isocenter. It is determined from the following equation 4 (7,22):

$$\varphi_A = \frac{\beta Q_n}{4\pi d_1^2} + \frac{5.4\beta Q_n}{2\pi S_r} + \frac{1.26 Q_n}{2\pi S_r} \quad (4)$$

Where Q_n is the apparent neutron source strength of neutrons emitted from the accelerator head for each Gy of X-rays absorbed at the isocenter, d_1 is the distance from the isocenter to the inner maze point A, S_r is the surface area of the treatment room and β is the transmission factor for neutrons that penetrate the head shielding. The Q_n values used in this work are taken from the literature (23).

Statistical analysis

A statistical analysis of data was carried out using IBM SPSS-23 software (IBM, USA) with an error of $\alpha=5\%$. A p-value less than 0.05 was considered to be statistically significant. The paired student's t-test was applied to verify if there is a significant difference between the obtained results.

RESULTS

Figure 2 illustrates the energy spectra of neutrons obtained by MCNP5 code at the isocenter for photon beam energies of 12, 15, 18, and 25 MV. It can be observed, that all spectra show an intense peak in the range of 200 keV to 1 MeV. This figure also shows a notable increase in fast and thermal neutron fluences as the beam energy increases exhibiting a most probable energy approximately at 0.5 MeV across all spectra which is consistent with the work of Facure *et al.* (24).

Table 1 compares the dose equivalent of neutrons obtained from Monte Carlo method, and those calculated by the analytical method of Wu-McGinley, in the absence of the shield door, at the maze entrance (point H in figure 1a). Additionally, this table includes measurements found in the literature (25).

Figures 4, 5, 6, and 7 show the simulated neutron spectra at the isocenter for photon beam energies of 12, 15, 18, and 25 MV respectively, in the three circumstances ((I), (II), and (III), figure 1b). The fluence of photoneutrons increases as the energy of the photon beam increases in all three scenarios.

These figures also show that the presence of a shield door has no significant impact on the neutron fluences at the isocenter. However, the use of the wall linings has greatly reduced the thermal and fast neutron fluences.

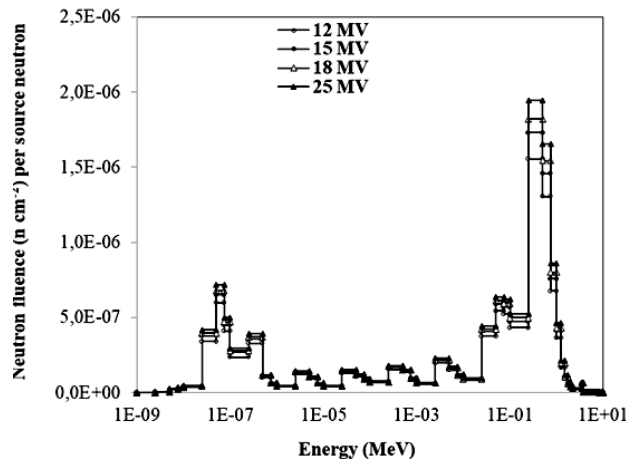


Figure 2. The neutron spectra assessed at the isocenter for photon beam energies of 12, 15, 18, and 25 MV in case (I) (without lining and without door).

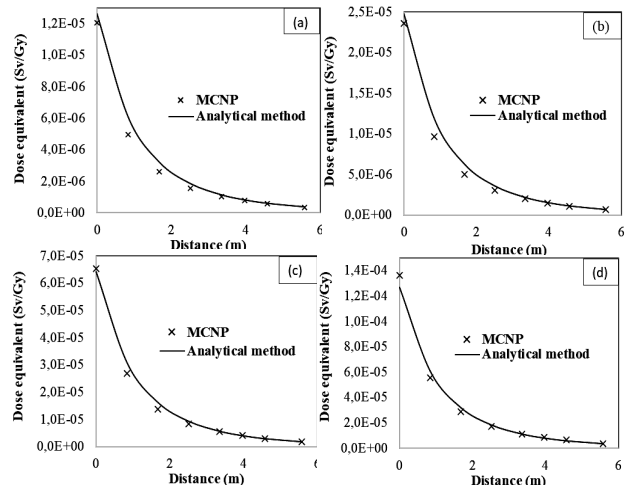


Figure 3. Comparison of the neutron dose equivalents obtained by MCNP simulation with those calculated using the Wu-McGinley analytical method. (a) for 12 MV photon beam, (b) for 15 MV photon beam, (c) for 18 MV photon beam, and (d) 25 MV photon beam.

Table 1. Comparison of the neutron dose equivalents at the maze entrance using MCNP and Wu-McGinley analytical methods, for photon beam energies of 12, 15, 18, and 25 MV.

Photon beam energy (MV)	Neutron dose equivalent ($H_{n,D}$) ($\mu\text{Sv/Gy}$)			p-value
	Analytical method	MCNP	Measured ($H_{n,D}$) (McGinley & Butker) ^[25]	
12	0.348	0.334 ± 0.014	-	0.100
15	0.681	0.649 ± 0.014	0.330 – 1.580	0.102
18	1.770	1.720 ± 0.014	0.400 – 5.500	0.123
25	3.480	3.650 ± 0.013	-	0.233

Table 2 summarizes our calculated dose equivalents of neutrons at the isocenter for the cases (I), (II), and (III) (Figure 1b), for photon beam energies of 12, 15, 18, and 25 MV. Our results show that the neutron dose equivalents increase as the

energy of the photon beam increases for all cases ((I), (II), and (III)).

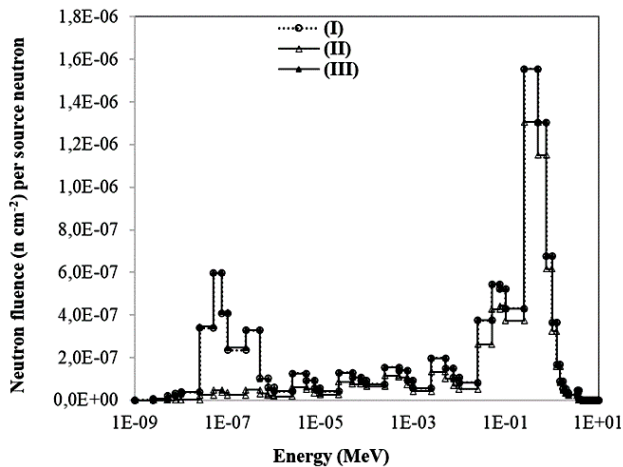


Figure 4. The neutron spectra simulated by MCNP at the isocenter for a photon beam energy of 12 MV. ((I): without door and without wall linings, (II): with wall linings, (III): with door (Figure 1b)).

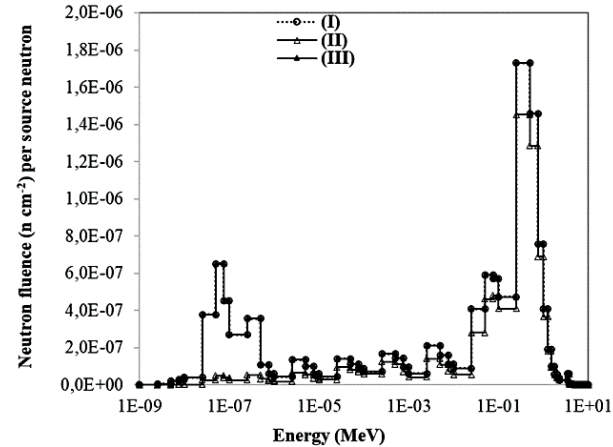


Figure 5. The neutron spectra simulated by MCNP at the isocenter for a photon beam energy of 15 MV. ((I): without door and without wall linings, (II): with wall linings, (III): with door (Figure 1b)).

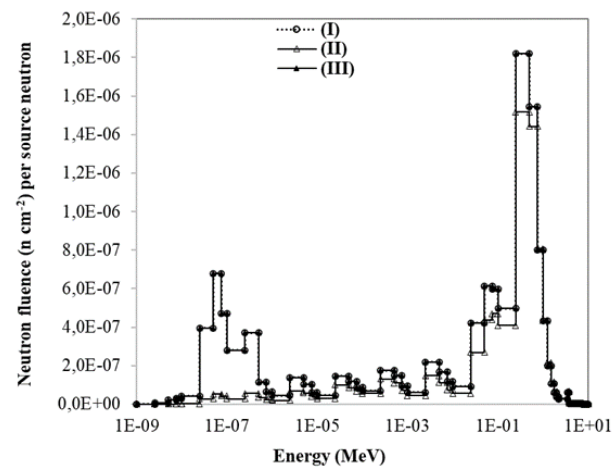


Figure 6. The neutron spectra simulated by MCNP at the isocenter for a photon beam energy of 18 MV. ((I): without door and without wall linings, (II): with wall linings, (III): with door (Figure 1b)).

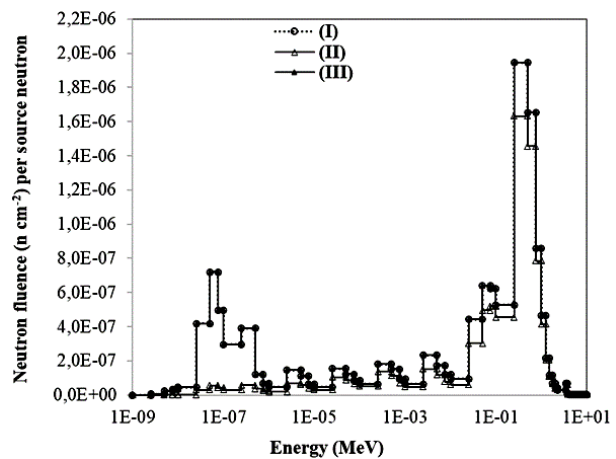


Figure 7. The neutron spectra simulated by MCNP at the isocenter for a photon beam energy of 25 MV. ((I): without door and without wall linings, (II): with wall linings, (III): with door (Figure 1b)).

Table 2. The neutron dose equivalents calculated at the isocenter, and the dose reduction in the presence of wall linings, for photon beam energies of 12, 15, 18, and 25 MV. ((I): without door and without wall linings, (II): with wall linings, (III): with door (figure 1b)).

Photon beam energy (MV)	Neutron dose equivalent ($H_{n,D}$) at the isocenter (mSv/Gy)			Reduction by the presence of wall linings (%)
	(I)	(II)	(III)	
12	0.263±0.001	0.228±0.001	0.263±0.001	13.0
15	0.516±0.001	0.450±0.001	0.516±0.001	12.8
18	1.430±0.001	1.340±0.001	1.430±0.001	6.1
25	2.980±0.001	2.610±0.001	2.980±0.001	12.6

Figure 8 illustrates four line charts that compare the dose equivalents of neutrons calculated by the MC method at various distances along the maze for the three cases (I), (II), and (III) (figure 1b) for photon beam energies of 12, 15, 18, and 25 MV.

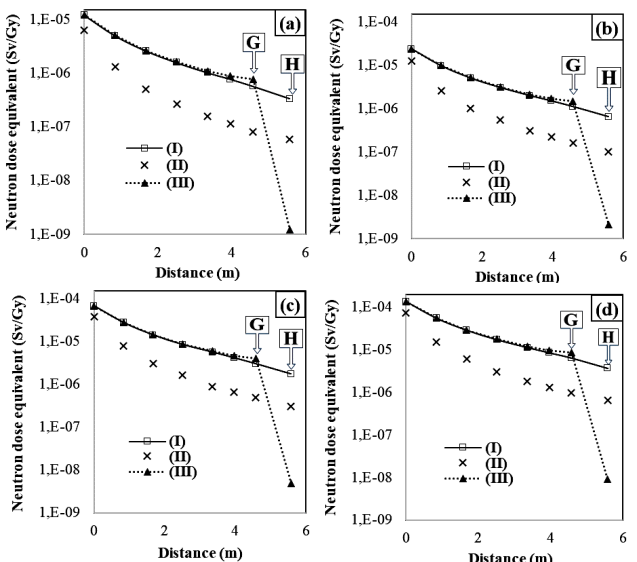


Figure 8. The neutron dose equivalents calculated along the maze from the inner entrance (point A) to the outer maze entrance (point H) ((a) for 12 MV photon beam, (b) for 15 MV photon beam, (c) for 18 MV photon beam, (d) for 25 MV photon beam). ((I): without door and without wall linings, (II): with wall linings, (III): with door).

Figure 9 shows a comparison between the capture gamma dose equivalents, determined through the MC method at various points along the maze, for the previous cases (I), (II), and (III), for photon beam energies of 12, 15, 18, and 25 MV. As we can see, the capture gamma doses decrease when moving towards the door entrance, for all cases. Additionally, this figure (dashed line) indicates an increased dose at point G with the addition of the door.

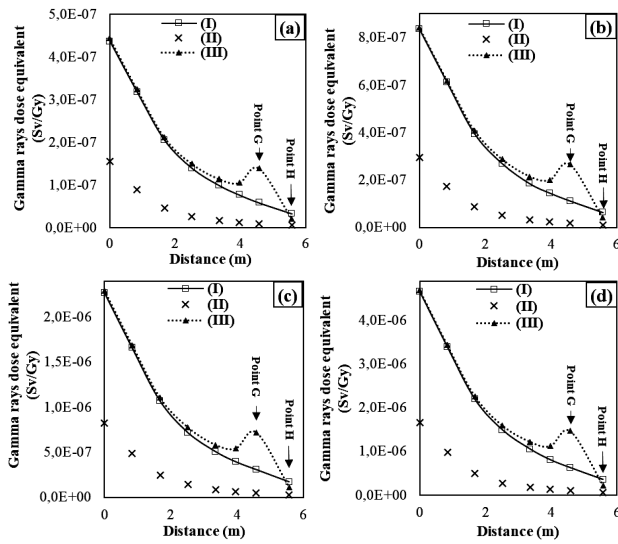


Figure 9. The capture gamma dose equivalents calculated along the maze (a) for 12 MV photon beam, (b) for 15 MV photon beam, (c) for 18 MV photon beam, (d) for 25 MV photon beam).

Figures 10, 11, 12, and 13 present the neutron energy spectra calculated at the outer maze entrance (point H in figure 1.a) for all photon beam energies in each considered case. In these figures the neutron fluences are of the order of 10^{-8} , 10^{-10} and 10^{-11} (neutron/cm²), for the cases (I), (II), and (III), respectively. It can be observed that the presence of the laminated shield door reduces both thermal and fast neutron fluences by up to 99%, at the outer maze entrance, for all photon beam energies. Whereas, the neutron absorption lining on the room walls provides up to 98% reduction for thermal neutrons and up to 79% reduction for fast ones, respectively.

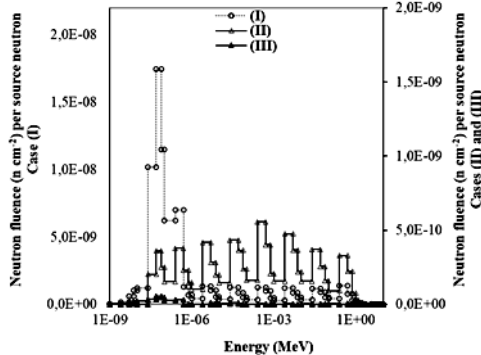


Figure 10. The neutron spectra calculated by MCNP at the maze entrance (point H, figure 1.a) for a photon beam energy of 12 MV. (I): without door and without wall linings, (II): with wall linings, (III): with door.

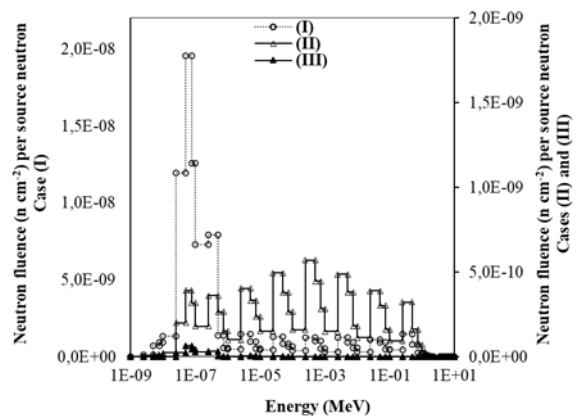


Figure 11. The neutron spectra calculated by MCNP at the maze entrance (point H, figure 1.a) for a photon beam energy of 15 MV. (I): without door and without wall linings, (II): with wall linings, (III): with door).

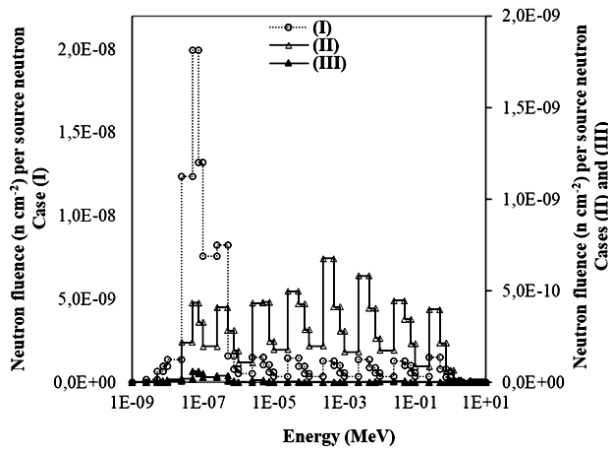


Figure 12. The neutron spectra calculated by MCNP at the maze entrance (point H, figure 1.a) for a photon beam energy of 18 MV. (I): without door and without wall linings, (II): with wall linings, (III): with door).

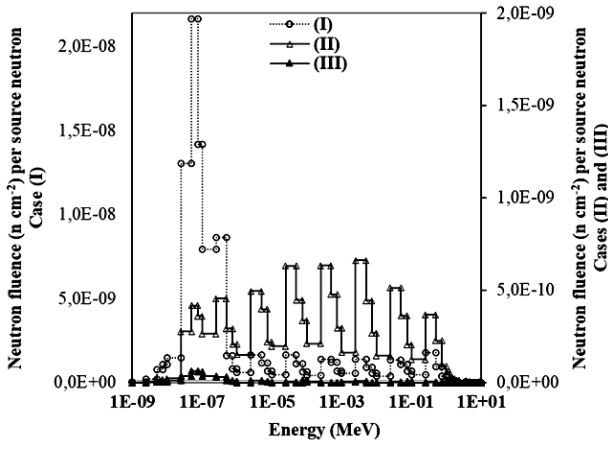


Figure 13. The neutron spectra calculated by MCNP at the maze entrance (point H, figure 1.a) for a photon beam energy of 25 MV. (I): without door and without wall linings, (II): with wall linings, (III): with door).

Table 3 compares the values of the neutron dose equivalents calculated at the maze entrance, for the three cases (I), (II), and (III) (Figure 1.b), and for photon beam energies of 12, 15, 18, and 25 MV.

Table 3. Comparison of neutron dose equivalents at the maze entrance, for the photon beam energies of 12, 15, 18, and 25 MV. ((I): without door and without wall linings, (II): with wall linings, (III): with door).

Photon beam energy (MV)	Neutron Dose equivalent ($\mu\text{Sv}/\text{Gy}$)			Reduction (%)	
	At the maze entrance			By the wall linings (II)	By the door (III)
	(I)	(II)	(III)		
12	0.334 \pm 0.014	0.058 \pm 0.045	1.210E-03 \pm 0.288	82.55	99.64
15	0.649 \pm 0.013	0.102 \pm 0.043	2.110E-03 \pm 0.278	84.35	99.67
18	1.720 \pm 0.013	0.302 \pm 0.041	4.880E-03 \pm 0.245	82.47	99.72
25	3.650 \pm 1.013	0.654 \pm 0.040	8.980E-03 \pm 0.121	82.08	99.75

Table 4 presents the total (neutron + gamma-ray) dose equivalent reduction calculated at the isocenter and at the maze entrance door (point H in figure 1.a) for the cases (I), (II), and (III). As we can see, the total dose is significantly reduced in the presence of wall linings and laminated shield door.

Table 4. Total dose equivalents calculated at the isocenter and at the outer maze entrance, for photon beam energies of 12, 15, 18, and 25 MV. (I): without door and without wall linings, (II): with wall linings, (III): with door.

Photon beam energy (MV)	Total dose equivalent (Neutron+ Gamma) (mSv/Gy)						Reduction (%)	
	At the isocenter			At the maze entrance			At the maze entrance	
	(I)	(II)	(III)	(I)	(II)	(III)	By the wall linings	By the door
12	0.265	0.230	0.265	3.670E-04	6.380E-05	2.260E-05	82.59	93.84
15	0.520	0.453	0.520	7.130E-04	1.120E-04	4.310E-05	84.32	93.96
18	1.440	1.350	1.440	1.890E-03	3.310E-04	1.160E-04	82.52	93.87
25	3.000	2.620	3.000	4.000E-03	7.150E-04	2.290E-04	82.15	94.29

DISCUSSION

In this work the effect of the laminated shield door and the wall linings, on the neutron and capture gamma doses in a radiotherapy room was investigated in order to determine the most adequate. The MCNP5 code was used to simulate the radiotherapy room of a medical linear accelerator operating at 12, 15, 18, and 25 MV. The calculations were performed in the absence and the presence of wall linings as well as a laminated shield door located at the maze entrance (cases (I), (II) and (III), figure1b). The effect of these shields was quantified in terms of dose equivalent reduction of both neutrons and capture gamma rays.

To verify the accuracy of our Monte Carlo simulation, we compared our MC simulated neutron dose equivalents (case (I)) with those evaluated by

Wu-McGinley analytical method (figure 3 and table 1). Our results indicate a strong agreement between the simulation values and those obtained through the analytical method. The relative error between the two methods was found to be less than 5%. In addition, the statistical analysis results (summarized in table 1) indicated that the p-values obtained from the two methods are greater than 0.05, which means that there is no significant difference between the calculated neutron dose equivalents. Furthermore, our simulated values (summarized in table 1) calculated for beam energies of 15 MV (0.649 $\mu\text{Sv}/\text{Gy}$) and 18 MV (1.720 $\mu\text{Sv}/\text{Gy}$) fall within the ranges of 0.330 to 1.580 $\mu\text{Sv}/\text{Gy}$ and 0.400 to 5.500 $\mu\text{Sv}/\text{Gy}$, respectively. These values were measured for Siemens and Varian linear accelerators by McGinley and Butker (25). Moreover, the neutron dose equivalent (table 2) for 15 MV (0.516 mSv/Gy) at the isocenter shows good agreement with the measured value of 0.59 mSv/Gy reported by Rivera *et al.* (26) for the 15 MV Varian LINAC.

Our results (summarized in table 1-2 and figures 4-7) showed that the photon beam energy has a significant impact on the neutron fluence and the dose equivalents. The neutron dose equivalent is higher for 25 MV than at energies of 12, 15 and 18 MV. This is attributed to the increase in the neutron source strength Q_n which increases with the beam energy as reported in literature (27). In addition, Zabihzadeh *et al.* (28) and Suliman *et al.* (29) had suggested in their studies that the increase of photon energy increases the probability of photoneutron interactions. Additionally, our investigation (illustrated in figure 2) shows that the fast neutrons were found to be the dominant component of the neutron spectra at the isocenter as reported by Naseri and Mesbahi (30). Furthermore, the shape of the calculated spectra at the isocenter for a photon beam energy of 15 MV (case (I) in figure 5) corresponds well with those measured by Chu *et al.* (31). This further confirms that our Monte Carlo simulations are reliable and can be used to accurately predict the neutron and capture gamma dose equivalents in radiotherapy rooms.

Once validated, the Monte Carlo simulation was used to assess the effectiveness of the shielding at the isocenter, of the laminated shield door and the wall linings (cases (II) and (III), figure1b). Our results (figures 4-7) showed that the wall linings prove to be more efficient, with a 16% reduction of fast neutron fluences and a remarkable 92% decrease for thermal neutrons at the isocenter. Incorporating paraffin wax infused with boron carbide into the room wall lining resulted in a reduction (at the patient plan) of up to 13% and 35.9% of the neutron and capture gamma dose equivalents, respectively, for all beam energies (table 2). However, the use of a laminated shield door has no significant effect on the neutron fluence and dose equivalents at the isocenter.

The effect of these shields on the neutron dose equivalent at maze entrance (point H in figure 1.a) was also investigated. Our results (figure 8 and table 3) show that the presence of the neutron shield in the lining of the radiotherapy wall rooms reduces the doses ($H_{n,D}$) along and at the maze entrance. However, a significant reduction is observed at the maze entrance, when the laminated shield door is added at the outer maze (point H in figure 1.a). According to the obtained data, the incorporation of wall linings and a laminated shield door reduce significantly the neutron dose equivalents by up to 84% and 99.75%, respectively. Gamma ray capture dose equivalents also showed significant reductions, with wall linings contributing up to 84.08% and the laminated shield door further reducing gamma ray exposure by 38.2% (figure 9). The statistical analysis confirmed the robustness of these findings (table 3), with p-values from cases (I), (II) and (III) all below 0.05, indicating clear distinctions in the neutron dose equivalents between case (I) and the other scenarios.

A similar shielding method as in our study reported by Wang *et al.*⁽¹²⁾ showed that the use of borated polyethylene (BPE) with 5% of boron to line the maze walls reduce the neutron dose by 41% and gamma dose by 59% at the maze entrance for a Varian 18 MV accelerator, as opposed to our study where we lined the entire walls of both the treatment room and the maze with paraffin wax incorporating boron carbide. This resulted in high dose reduction of 82.47% and 83.03% for the neutron and capture gamma doses, respectively, for 18 MV photon beam energy (table 3). It has also been demonstrated in the study of Ghassoun *et al.*⁽¹¹⁾ that paraffin wax with boron carbide is highly effective in reducing the neutron and gamma doses for 18 MV medical linear accelerators.

In our work, the use of laminated shield has shown a high reduction of the neutron dose of 99.67% for 15 MV at the maze entrance (table 3), compared to the study performed by Kim *et al.*⁽³²⁾, who achieved a reduction of 96.2% by using lead-BPE-lead for their laminated shield door. This difference can be attributed to the simulated BPE thickness, which is 10.2 cm for us compared to 4 cm in the study of Kim *et al.*⁽³²⁾.

The effectiveness of these shields on the total (neutron + gamma-ray) dose equivalent, at the isocenter and at the maze entrance, was also investigated. Our results (summarized in table 4) show that the wall linings decrease the dose at the isocenter by up to 13.16%. However, the presence of the laminated shield door has no significant effect on the total dose. The obtained results also show that the total dose equivalent reduction at maze entrance in the presence of the wall linings decrease by up to 84.32%. Whereas, the reduction is up to 94.29% when the laminated shield door is added at the outer maze entrance.

The reduction is attributed to neutron moderation to thermal energies through elastic scattering, due to the presence of hydrogen in the wax used for wall linings (case (II)), and in the polyethylene for the laminated shield door (case (III)). These thermal neutrons are then captured by boron-10 (^{10}B). This reduces the magnitude of the thermal neutron fluences and also decreases the prompt gamma ray dose equivalents.

Because of its composition, the shield door is more adequate to reduce the dose at the maze entrance. In addition, both lead and steel are effective materials for attenuating capture gamma rays.

This study offers valuable insights into radiation protection. Such insights are crucial for optimizing shielding design and ensuring enhanced radiation protection for patients and healthcare professionals in clinical settings. In this work, we were limited to calculating the dose at the isocenter and at the maze entrance of a medical accelerator (Saturne 43). However, the goal can be further extended to study the effect of the presence of the wall linings and shield door on the dose distribution in the vicinity of high energy radiotherapy facilities for different photon beam energies and other medical accelerators.

CONCLUSION

Base on this study, it can be concluded that the use of neutron shielding material in the lining of radiotherapy room walls is more appropriate for protecting patients from radiation exposure. However, the use of a shield door is more effective in protecting the staff and the general public.

ACKNOWLEDGEMENT

None.

Funding: No funding from any entity was allocated.

Conflicts of Interest: The authors declare that they have no conflicts of interest.

Authors' contribution: All authors had complete access to the study data and assumed responsibility for the data's integrity and accuracy in the analysis. All authors were involved in the study and preparation of manuscript equally.

REFERENCES

1. Ghiasi H and Mesbahi A (2012) A new analytical formula for neutron capture gamma dose calculations in double-bend mazes in radiation therapy. *Reports of Practical Oncology and Radiotherapy*, **17**(4): 220-5.
2. Alem-Bezoubiri A, Bezoubiri F, Badreddine A, Mazrou H, Lounis-Mokrani Z (2014) Monte Carlo estimation of photoneutrons spectra and dose equivalent around an 18MV medical linear accelerator. *Radiation Physics and Chemistry*, **97**: 381-92.
3. Banaee N, Goodarzi K, Nedaei HA (2021) Neutron contamination in radiotherapy processes: a review study. *J Radiat Res*, **62**(6): 947-54.

4. Rajesh KR, Ganapathi Raman RG, Musthafa MM, Midhun CV, Joseph N (2020) A passive method for absolute dose evaluation of photoneutrons in radiotherapy. *Int J Radiat Res*, **18**(1): 173-178.

5. Ghiasi H (2014) Monte Carlo characterizations mapping of the (γ ,n) and (n, γ) photonuclear reactions in the high energy X-ray radiation therapy. *Reports of Practical Oncology and Radiotherapy*, **19**(1): 30-6.

6. NCRP, National Council on Radiation Protection and Measurements (2006) Structural shielding design and evaluation for megavoltage X - and gamma-ray radiotherapy facilities. *NCRP Report No. 151* NCRP, Bethesda, MD.

7. IAEA, The International Atomic Energy Agency (2006) Radiation protection in the design of radiotherapy facilities. *Reports series No. 47*. Vienna.

8. Yücel H, Çobanbaş I, Kolbaşı A, Yüksel AÖ, Kaya V (2016) Measurement of photo-neutron dose from an 18-MV medical linac using a foil activation method in view of radiation protection of patients. *Nuclear Engineering and Technology*, **48**(2): 525-32.

9. Ghassoun J (2015) The effect of the presence of the patient on the particles dose estimations in high energy linear accelerator mazes. *Int J Can Ther Oncol*, **3**(3): 3321.

10. Ghassoun J and Senhou N (2012) The evaluation of neutron and gamma ray dose equivalent distributions in patients and the effectiveness of shield materials for high energy photons radiotherapy facilities. *Appl Radiat Isot*, **70**(4): 620-4.

11. Ghassoun J, Senhou N, Jehouani A (2011) Neutron and photon doses in high energy radiotherapy facilities and evaluation of shielding performance by Monte Carlo method. *Ann Nucl Energy*, **38**(10): 2163-7.

12. Wang X, Esquivel C, Nes E, Shi C, Papanikolaou N, Charlton M (2011) The neutron dose equivalent evaluation and shielding at the maze entrance of a Varian Clinac 23EX treatment room. *Med Phys*, **38**(3): 1141-9.

13. Afkham Y, Mesbahi A, Alemi A, Zolfagharpour F, Jabbari N (2020) Design and fabrication of a Nano-based neutron shield for fast neutrons from medical linear accelerators in radiation therapy. *Radiat Oncol*, **15**: 105.

14. Mesbahi A, Ghiasi H, Mahdavi SR (2010) Photoneutron and capture gamma dose equivalent for different room and maze layouts in radiation therapy. *Radiat Prot Dosim*, **140**(3): 242-49.

15. X-5 Monte Carlo Team (2005) MCNP-A general Monte Carlo N-particle transport code, Version 5. Los Alamos National Laboratory report LAUR-03-1987.

16. NCRP, National Council on Radiation Protection and Measurements (1971) Protection against neutron radiation. *Report No. 38* Bethesda, Maryland.

17. ICRP, International Commission on Radiological Protection (1996) Conversion coefficients for use in radiological protection against external radiation. *ICRP Publication 74*, **26**(3-4). ICRP, Ottawa, ON.

18. Simmons G (1978) Book Review: Structural shielding design and evaluation for medical use of X-Rays & gamma rays of energies up to 10 MeV. NCRP Report No. 49. *Journal of Nuclear Medicine*, **19**(2): 228.

19. Eller LR (2012) An investigation on photoneutron production from medical linear accelerator. M.S. Oregon State University.

20. Tosi G and Torresin A (1991) neutron measurements around medical electron accelerators by active and passive detection techniques. *Med Phys*, **18**(1): 54-60.

21. Wu RK and Patton HM (2003) Neutron and capture gamma along the mazes of linear accelerator vaults. *J Appl Clin Med Phys*, **4**(2): 162-71.

22. Ivković A, Faj D, Galić S, Karimi A, Kasabašić M, Brkić H (2020) Accuracy of empirical formulas in evaluation of neutron dose equivalent inside the 60Co vaults reconstructed for medical linear accelerators1. *Int J Radiat Res*, **18**(1): 99-107.

23. Followill DS, Stovall MS, Kry SF, Ibbott GS (2003) Neutron source strength measurements for Varian, Siemens, Elekta, and General Electric linear accelerators. *J Appl Clin Med Phys*, **4**(3): 189-194.

24. Facure A, Falcão RC, Silva AX, Crispim VR, Vitorelli JC. (2005) A study of neutron spectra from medical linear accelerators. *Appl Radiat Isot*, **62**(1): 69-72.

25. McGinley PH, Butker EK (1991) Evaluation of neutron dose equivalent levels at the maze entrance of medical accelerator treatment rooms. *Med Phys*, **18**(2): 279-81.

26. Rivera J C, Falcao R C, deAlmeida C E (2008) The measurement of photoneutron dose in the vicinity of clinical linear accelerators. *Radiation Protection Dosimetry*, **130**(4): 403-409.

27. Mohammadi N, Miri-Hakimabad SH, Rafat-Motavalli L (2014) A Monte Carlo study for photoneutron dose estimations around the high-energy linacs. *J Biomed Phys Eng*, **4**(4): 127-40.

28. Zabihzadeh M, Ay MR, Allahverdi M, Mesbahi A, Mahdavi SR, Shahriari M (2009) Monte Carlo estimation of photoneutrons contamination from high-energy X-ray medical accelerators in treatment room and maze: A simplified model. *Radiat Prot Dosimetry*, **135**(1): 2.

29. Suliman II, Khouqueer GA, Mayhoub FH (2023) Photoneutrons and Gamma Capture Dose Rates at the Maze Entrance of Varian True-Beam and Elekta Versa HD medical linear accelerators. *J Toxics*, **11**(1): 78.

30. Naseri A and Mesbahi A (2010) A review on photoneutrons characteristics in radiation therapy with high-energy photon beams. *Rep Pract Oncol Radiat*, **15**(5): 138-44.

31. Chu WH, Lan JH, Chao TC, Lee CC, Tung CJ (2011) Neutron spectrometry and dosimetry around 15 MV linac. *Radiation Measurements*, **46**(11): 1741-1744.

32. Kim YN, Choi SH, Jeong K, Kim JY, Lee CG, Seong J, Kim CH (2008) A study on optimization of photoneutron shielding in a medical accelerator room by using Monte Carlo simulation. *Journal of Nuclear Science and Technology*, **45**(sup5): 50-53.